18TH WORLD CONFERENCE ON EARTHQUAKE ENGINEERING
WCEE2024
MILAN

MILAN, ITALY
30TH JUNE - 5TH JULY 2024

www.wcee2024.it

# SEISMIC RESILIENCE OF COMPOSITE RCS SPECIAL MOMENT FRAMES BASED ON FEMA P695 METHODOLOGY

M.H. Habashizadeh[1], N. Talebian[2], D. Miller[3], H. Karampour[4], D. Forcellini[5], A. Ghanbaripour[6]

[1] Department of Civil Engineering, Islamic Azad University- Marand Branch, Marand, Iran, m_habashi@marandiau.ac.ir

[2] Faculty of Society and Design, Bond University, Gold Coast, Australia, ntalebia@bond.edu.au

[3] Faculty of Society and Design, Bond University, Gold Coast, Australia, dmiller@bond.edu.au

[4] School of Engineering and Built Environment, Griffith University, Gold Coast, Australia, h.karampour@griffith.edu.au

[5] Department of Civil and Environmental Engineering, Università di San Marino, San Marino, davide.forcellini@unirsm.sm

[6] Faculty of Society and Design, Bond University, Gold Coast, Australia, aghanbar@bond.edu.au

**Abstract**: *Hybrid reinforced concrete-steel (RCS) systems, which combine steel (S) beams and reinforced concrete (RC) columns, offer more practical and cost-effective benefits than conventional steel and concrete moment frames due to their efficient use of materials. Under the current International Building Code (IBC) and ASCE/SEI 7-05, RCS systems are classified as special moment frames and a response modification (R) factor of 8 is considered in their seismic design. This research aims to evaluate the seismic resilience and R factor of RCS composite special moment frames following the methodology provided in FEMA P695. 3-bay multi-story (3, 5, 10 and 15) archetypes were designed to conduct incremental dynamic analysis (IDA) in OpenSEES software. The nonlinear response of a typical RCS connection is implemented in the archetypes. The fragility curves were obtained to investigate the safety margin against collapse outlined by FEMA P695. The results showed that the evaluated archetypes meet the FEMA P695 acceptance criteria for an R factor of 8.*

## 1 Introduction

Due to the efficient material combination used, steel-concrete composite structures are more cost-effective than typical steel or concrete structures. Structural system made of reinforced concrete columns and steel beams, or RCS system, is a hybrid moment-resisting frame system that is increasingly being used for mid- to high-rise buildings. The advantages of traditional steel and concrete frames are combined in this kind of system. RC columns offer significantly improved lateral stiffness, improved structural damping, and are more economical and efficient in compression. Lateral stiffness becomes more crucial in tall buildings as drift requirements become a key element of building design. When steel beams are used instead of concrete ones, the dead load and foundation expenses of the structure can be significantly decreased, and the overall ductility and energy dissipation capacity can be improved (Nishiyama et al. 2004, Li et al. 2011). Steel beams also have the advantage of being able to accommodate bigger column-free zones because of their superior bending capability compared to their RC counterparts. Furthermore, a composite floor system made of a concrete slab

and steel beams is more effective than traditional concrete precast subassemblies and provide a larger cost benefit over concrete formwork when it comes to constructability (Griffis 1992). There are two primary forms of RCS connections: "beam-through" and "column-through," with the former being the most popular because of its improved ductility (Cordova 2005). A typical beam-through RCS connection is depicted in Figure 1.a, where steel beam continuously passes through RC columns to create a composite connection. The RCS connection is normally made up of the following components: (i) longitudinal steel reinforcement of the RC column; (ii) stiffened steel band plates (SBP), which are wrapped around the column in the connection and used to confine concrete in the connection to avoid bearing failure; (iii) face bearing plates (FBP) are welded to the steel beam and used to actuate the concrete between the beam flanges, and (iv) U-shaped stirrups passing through holes in the web of the steel beam (Cordova 2005). The performance of RCS moment connections, with multiple joint details and RCS frames, has been extensively studied. Experimental and numerical studies have demonstrated the superior behaviour and seismic performance of RCS frames.

Accurately determining the response modification factor, or R, is essential to predict the seismic behaviour of a structural system during earthquake action. Questions have been raised regarding the reliability of R values determined by the typical method utilised by seismic design standards such as the International Building Code (IBC) (2006), in light of the unexpected seismic performance of various structural systems in buildings during earthquakes. FEMA P695 (2009) has recommended a global technique that addresses this issue and assesses the accuracy of the R factors. This is predicated on measuring the existing uncertainties in the process to achieve a reliable seismic performance, subject to the maximum considered earthquake (MCE).

The primary goal of this paper is to examine seismic resilience and R factor of RCS composite frames using the FEMA P695 technique. Using the Open System for Earthquake Engineering Simulation (OpenSEES) software, a series of 3-bay and multi-story (3, 5, 10, and 15) archetypes were modelled for this purpose. Using the record-set of ground motions provided in FEMA P695, incremental dynamic analysis (IDA) was used to assess the resilience and collapse performance of the frames.

## 2 RCS connection and RCS frame response

Sheikh (1987), Deierlein (1988), Sheikh et al. (1989), and Kanno (1993) conducted some of the earliest primary research, examining the strength and stiffness of inner beam-through RCS connections under cyclic and monotonic loads with different connection features. The findings identified two failure mechanisms: (i) bearing failure due to high bearing stress-induced concrete crushing immediately above and below the steel beam flanges, and (ii) shear failure due to the yielding of the steel beam's web. The joint strength model that emerged from these investigations formed the basis for the 1994 guidelines published by ASCE for the design of RCS composite connections in areas with low to moderate seismicity. In their studies of the seismic performance, design, and modelling of RCS connections, Bracci et al. (1994), Kanno and Deierlein (1996 and 2002), Bugeja et al. (2000), Parra-Montesinos and Wight (2001), Parra-Montesinos et al. (2003), Kuramoto and Nishiyama (2004) suggested several changes to the revised 1994 ASCE guidelines. A few of the noteworthy results included addressing the variations between exterior and interior joint designs and the application of RCS frames in areas prone to high seismic activity. Considering these investigations, updated recommendations for the design of RCS composite joints were developed by Cordova (2005).

Habashizadeh (2011), Habashizadeh et al. (2013) and Alizadeh et al. (2013) investigated RCS connections under cyclic loads and developed 3D Finite Element Method (FEM) modelling of the connections. More recently, new RCS connections with superior seismic performance have been proposed, as depicted in Figure 1. Alizadeh et al. (2015) tested a novel RCS joint detail with additional bearing plates (ABP) and wider FBPs, as shown in Figure 1.b, and reported improved shear and bearing strength. Doost and Khaloo (2021) proposed a new joint detail and experimentally investigated the seismic behaviour of two half-scale RCS connections with a precast RC column. The proposed RCS joint detail include an embedded steel web panel and extended face bearing plates with stiffener attached to beam flange, as shown in Figure 1.c. The steel beams were welded to extended steel plates connected to a steel web panel. This led to a notable improvement in the panel zone's shear strength and a decrease in joint deformation. Using a through-plate embedded in the RC column as shown in Figure 1.d, Eghbali and Mirghaderi (2017) experimentally tested a new RCS joint design and reported that the through-plate resulted in an increased strength and steady hysteretic behaviour. Mirghaderi et al. (2016) examined the seismic performance of a new RCS connection, which consists of

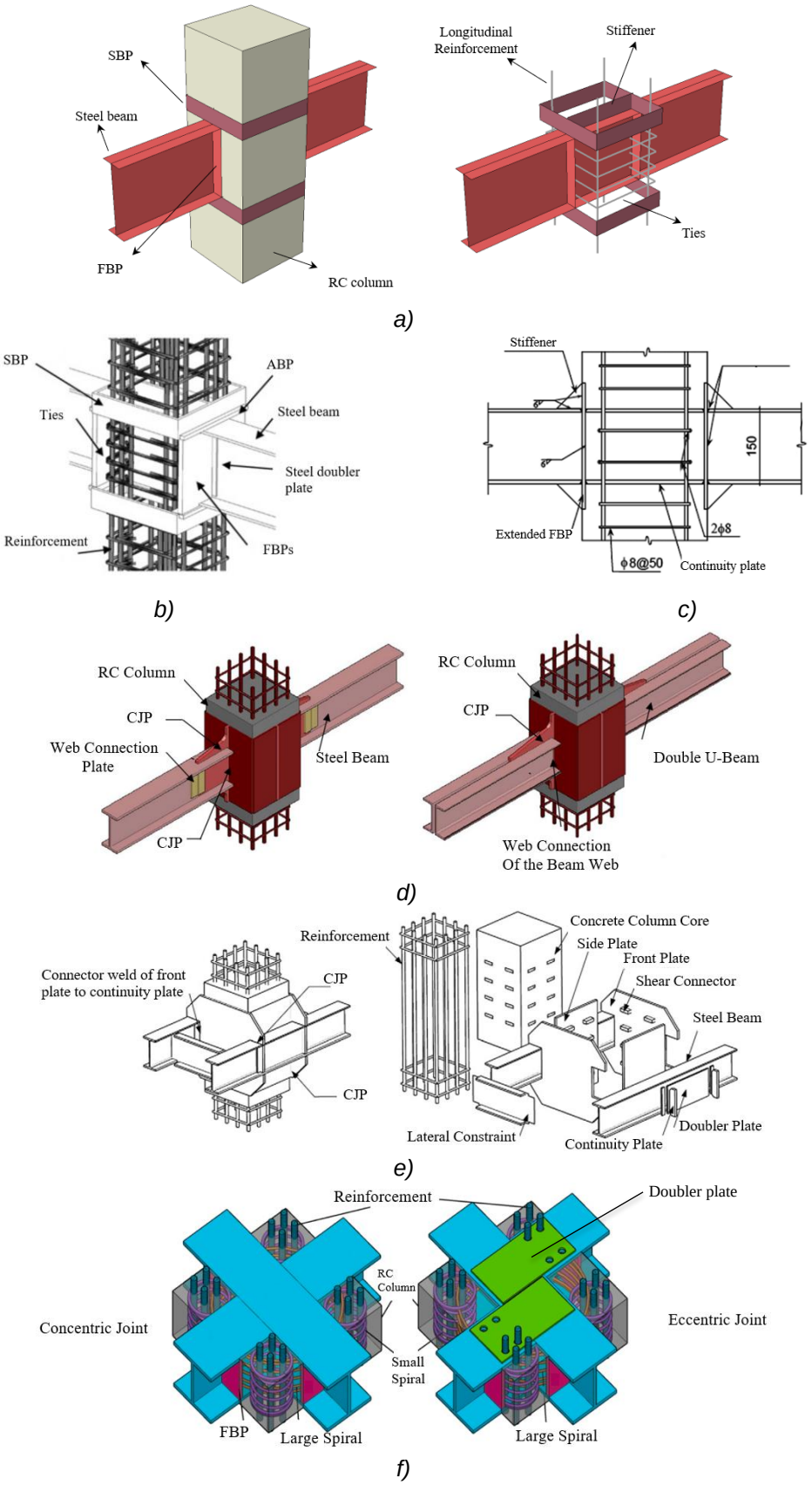


*Figure 1. RCS connections – a) Typical RCS joint (Cordova, 2005), b) RCS joint with ABP and wider FBP (Alizadeh et al., 2015), c) RCS joint with an embedded steel web panel and extended FBPs (Doost and Khaloo, 2021), d) RCS joint with a through-plate (Eghbali and Mirghaderi, 2017), e) RCS Joint with two parallel beams (Mirghaderi et al., 2016), f) RCS joint with spiral reinforcement (Ou et al., 2022).*

two parallel steel beams that are welded to steel cover plates enclosing the RC column and run from both sides of the column, as depicted in Figure 1.e. The experimental results showed that the proposed connection exhibits stable hysteretic response. Ou et al. (2022) experimentally tested a new high strength RCS joint with beams concentrically or eccentrically connected to the connection. The beams were connected by complete joint penetration groove welds (CJP). For joint reinforcement, a five-spiral configuration was employed, considering the confinement effect from FBPs. Additionally, doubler plates were utilized to reinforce the eccentric beam flanges, featuring predrilled holes for the passage of column longitudinal reinforcement, as demonstrated in Figure 1.f.

A significant number of experimental and numerical studies have been conducted on the response of RCS frames (Noguchi and Uchida (2004), Liang and Parra-Montesinos (2004), Wu et al. (2009), Chou and Chen (2010), Farahmand Azar et al. (2013)). A full-scale 3-story, 3-bay RCS frame was evaluated under quasi-static and pseudo-dynamic loading in a US-Taiwan collaboration (Chen et al. 2004, Cordova et al. 2004). Based on strong column–weak beam (SCWB) requirements in accordance with IBC (2006), the frame was built for a high seismic zone. Pseudo-dynamic loading was applied using four carefully chosen strong ground motions. The experiment demonstrated that the RCS frame exhibited strong seismic performance and met the criteria for collapse prevention. Cordova (2005) and Cordova et al. (2004) created a numerical model to represent the two primary RCS connection failure scenarios. The produced model was then utilized to replicate the behaviour of the tested full-scale RCS frame. The tested frame's numerical results agreed well with the experimental findings. More recently, Men et al. (2015) conducted an experimental evaluation of a two-bay, two-story RCS frame and found that it exhibited superior deformation capacity, outstanding seismic behaviour, and a substantially bigger displacement ductility coefficient than regular concrete or steel structures. Li et al. (2020) conducted an experimental study to test the seismic performance of three RCS frames. The study constructed finite element models to replicate the behaviour of the frames and proposed a plastic limit analysis approach to assess the lateral capacity of the tested frames.

## 3 FEMA P695 methodology to determine the R factor of RCS frames

### 3.1 FEMA P695 methodology

The FEMA P695 method is based on a trial process wherein the initial R factor is determined based on data that has already been collected regarding the structural system under investigation. For conducting nonlinear studies, structural models, or archetypes, are utilised that represent all the attributes of the system under investigation. To guarantee the reliability of the outcomes, the technique takes into consideration the uncertainty values pertaining to record-to-record variability, test data, design, and modelling needs. Based on the mean value of the collapse capacities of the studied archetypes and the collapse margin ratio, a probabilistic technique is used to evaluate the R factor in the design. The collapse margin ratio which represents the building's ability to withstand collapse over its design limit, is calculated as the ratio of the collapse capacities to MCE.

### 3.2 Archetype modelling and design

In this study, the same numerical approach as in Cordova (2005) was employed, and the tested full-scale 3-story, 3-bay RCS frame was remodelled to verify that the numerical response was consistent with the experimental results. To calculate the R factor, four RCS frames with four different number of stories (3, 5, 10, and 15) were analysed in the current study. The frames were selected from a hypothetical commercial RCS building. The examined RCS models, with a story height of 4.2 m, are shown in Figure 2. The steel beams and reinforced concrete columns were designed in accordance with AISC 360-16 (2016) and ACI 318-19 (2019), respectively. The typical beam-through RCS connection, as illustrated in Figure 1.a and utilised by Cordova (2005), was designed and used in all structural models. For instance, the member sections of the 3 story RCS frame are shown in Table 1. The commercial RCS building's design loads were determined in compliance with ASCE/SEI 7-05 (2006). A dead load of 560 kg/m$^2$ for the roof and 660 kg/m$^2$ for each floor was considered. Other than the roof level, the live load was taken to be 250 kg/m$^2$. At the roof level, the snow load was calculated to be 150 kg/m$^2$ for all frames. For all beams, steel with an ultimate stress of 520 MPa and a yield stress of 360 MPa was utilised. These values were 560 MPa and 400 MPa for steel reinforcement, respectively. The compressive strength of concrete was taken to be 28 MPa. In compliance with ASCE/SEI 7-05 (2006), drift control of the RCS frames was carried out to ensure that every model adhered to the permitted story drift. The columns of all frames were designed to satisfy the Strong-Column Weak-Beam (SCWB) criterion.

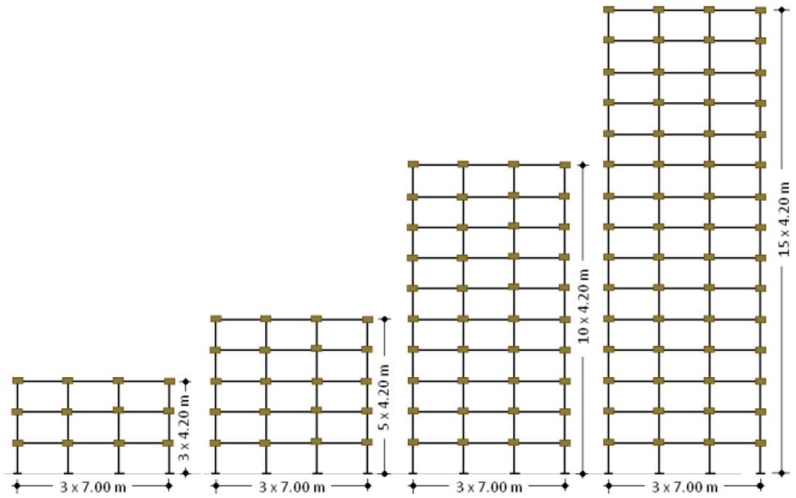


*Figure 2. Elevation view of the investigated RCS frames.*

*Table 1. Member sizes and input parameters of the RCS connections for 3-story frames*

| Story | Beam | Column | RCS Connection | Bearing failure | | Shear failure | |
|---|---|---|---|---|---|---|---|
| | | | | $M_{vb}$ (N.mm) | $K_{eb}$ (N.mm/rad) | $M_{ps}$ (N.mm) | $K_{es}$ (N.mm/rad) |
| 1 | W500×200 | C600×600-12Ø30 | C600-W500 (Ext.) | 1.58E+09 | 4.17E+11 | 1.19E+09 | 2.97E+11 |
| | | | C600-W500 (Int.) | 1.82E+09 | 5.30E+11 | 1.72E+09 | 4.67E+11 |
| 2-3 | W400×170 | C600×600-12Ø30 | C600-W400 (Ext.) | 1.23E+09 | 3.05E+11 | 8.14E+08 | 1.94E+11 |
| | | | C600-W400 (Int.) | 1.36E+09 | 3.64E+11 | 1.15E+09 | 2.92E+11 |
| | | | C600-W400 (Ext.)-Roof | 1.23E+09 | 2.83E+11 | 8.14E+08 | 1.83E+11 |
| | | | C600-W400 (Int.)-Roof | 1.36E+09 | 3.30E+11 | 1.15E+09 | 2.70E+11 |

Table 5 presents the seismic design parameters based on ASCE/SEI 7-05 (2006) and FEMA P695 (2009). For the analysis, the R value was taken to be 8, as recommended by IBC (2006) and ASCE/SEI 7-05 (2006) for special moment frames.

### 3.3 Modelling of RCS connections

The nonlinear beam-column element in OpenSEES was used to model the reinforced concrete columns and steel beams. Uniaxial material Concrete02 was used to simulate the confined and unconfined regions of the reinforced concrete columns. Uniaxial material Steel02 was used to represent the steel beams and steel reinforcement in columns. The behaviour of the RCS connections was replicated using Element Joint2D in OpenSEES. Joint size is equivalent to the width of the concrete column and the depth of the steel beam. A schematic view of this element is shown in Figure 3. To replicate the shear and bearing failure mechanisms, two nonlinear rotational springs were incorporated in series at the element's centre node. Figure 4 depicts the idealised moment-rotation relationship (Cordova 2005) used to model the shear failure in the web of the steel beams. The initial stiffness of shear spring was calculated based on Kanno's (1993) recommendations as:

$$K_{es} = \frac{2M_{ps}}{\theta_{so}}, \theta_{so} = 0.01 - 0.0067\sqrt{p} \quad (1)$$

where $K_{es}$ is the initial stiffness of the shear failure, $M_{ps}$ is the moment capacity of the RCS joint in shear failure, $\Theta_{so}$ is rotation at which the applied moment is equal to $M_{ps}$, and $p$ is ratio of the applied axial force to the axial capacity of the column. $M_{ps}$ is calculated in accordance with equations outlined in the updated ASCE guidelines (1994) and Cordova (2005). *Uniaxial material Steel02* is also employed to model the shear failure using $M_{ps}$ and $K_{es}$ instead of $F_y$ and $E$, respectively. Figure 5 illustrates the idealised Hysteretic material model (Cordova

*Table 2. Seismic design parameters*

| Design parameters | Values |
|---|---|
| Importance factor | 1 |
| Seismic design category (SDC) | $D_{max}$ |
| Site class | D |
| Initial response modification factor ($R$) | 8 |
| Initial deflection amplification factor | 5.5 |
| $S_1$ (g) | 0.6 |
| $S_s$ (g) | 1.5 |
| $F_a$ | 1 |
| $F_v$ | 1.5 |
| $S_{D1}$ (g) | 0.6 |
| $S_{Ds}$ (g) | 1 |

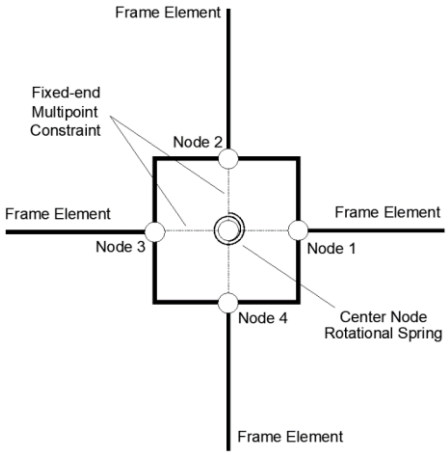


*Figure 3. Joint2D element in OpenSEES.*

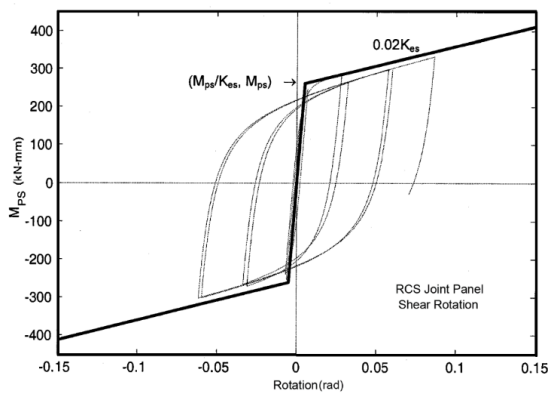


*Figure 4. Idealized moment-rotation relationship for shear failure mechanism in the web of the steel beam (Cordova 2005).*

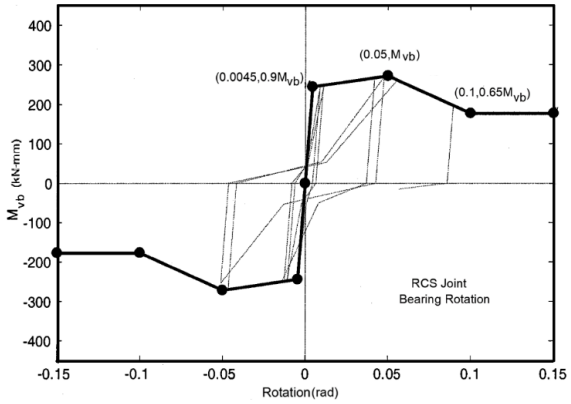


*Figure 5. Idealized moment-rotation relationship for bearing failure mechanism in the RCS connection (Cordova 2005)*

2005) to represent the bearing failure caused by the crushing of the concrete in the joint region. The initial stiffness of the bearing spring is determined according to the recommendations by Kanno (1993) as:

$$K_{eb} = \frac{2M_{vb}}{\theta_{bo}}, \theta_{bo} = 0.01 - 0.008\sqrt{p} \quad (2)$$

where $K_{eb}$ denotes the initial stiffness of the bearing failure, $M_{vb}$ is the moment capacity of the RCS joint in bearing, and $\Theta_{bo}$ is the rotation at which the applied moment is equal to $M_{vb}$. $M_{vb}$ is also calculated in accordance with equations outlined in the updated ASCE guidelines (1994) and Cordova (2005). For instance, the input parameters to represent shear and bearing failure for the interior and exterior joints of 3 story RCS frame are also shown in Table 1. A leaning column was pinned to the base and connected to each model using rigid truss links at floor level to account for the P-Δ effect caused by gravity loads. A 5% Rayleigh damping was assumed.

## 4 Nonlinear incremental dynamic analysis

Using the approach described in FEMA P695, nonlinear incremental analysis (IDA) was performed on all archetypes to determine the median collapse capacity ($S_{CT}$) and the collapse margin ratio (CMR). To conduct the IDA studies, 22 pairs of ground motion records prescribed by FEMA P695 are utilised. The records are scaled to ensure their mean spectra match the MCE spectrum corresponding to SDC $D_{max}$ at the fundamental period, after first being normalised by their respective peak ground velocities (PGV). SDC $D_{max}$ is the seismic design category used in high-seismic-risk areas. Table 3 provides the main characteristics of the records and normalization factors. The mean spectra of the normalised pre-defined ground motions are shown in Figure 6. In IDA analysis, the intensity was first increased at fixed steps, and then the steps were gradually reduced close to failure to obtain a more accurate seismic response. The global dynamic instability when the archetypes collapse (the IDA response forms a plateau) and the interstory drift limit of 4% for special moment frames, as specified by ANSI/AISC 341-10 (2010), are the two failure criteria used to evaluate the R factor of the RCS systems. Previous studies also indicate that the yielding of steel beams in RCS frames initiates at a 4% interstory drift (Cordova 2005, Li et al. 2020). Figure. 7 displays the IDA curves of the archetypes along with the 16th, 50th, and 84th percentile curves. 5% damped spectral acceleration at the archetypes' fundamental period was used for the RCS frames.

The collapse safety of the models was assessed by computing the collapse margin ratios, CMR and $CMR_{4\%}$, for both global and local criteria to evaluate the R factor. A higher collapse margin ratio indicates a higher likelihood of safety against collapse in the event of a seismic event, and is given by:

$$CMR(CMR_{(4\%)}) = \frac{S_{CT}(S_{CT(4\%)})}{S_{MT}} \quad (3)$$

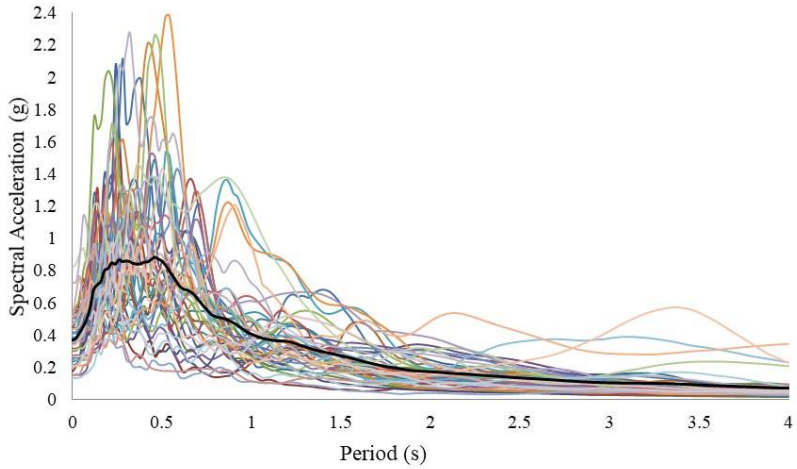


*Figure 6. Median spectra of the normalized ground motions prescribed in FEMA P695*

*Table 3. Ground motions prescribed in FEMA P695*

| ID | Location | Year | Epicenter (km) | $PGA_{max}$ (g) | Magnitude | Normalization factor |
|---|---|---|---|---|---|---|
| 1 | Northridge | 1994 | 13.3 | 0.53 | 6.7 | 0.62 |
| 2 | Northridge | 1994 | 26.5 | 0.52 | 6.7 | 0.85 |
| 3 | Duzce Turkey | 1999 | 41.3 | 0.82 | 7.1 | 0.63 |
| 4 | Hector Mine | 1999 | 26.5 | 0.37 | 7.1 | 1.08 |
| 5 | Imperial Valley | 1979 | 33.7 | 0.34 | 6.5 | 1.28 |
| 6 | Imperial Valley | 1979 | 29.4 | 0.40 | 6.5 | 0.98 |
| 7 | Kobe Japan | 1995 | 8.7 | 0.53 | 6.9 | 1.01 |
| 8 | Kobe Japan | 1995 | 46 | 0.26 | 6.9 | 1.15 |
| 9 | Kocaeli Turkey | 1999 | 98.2 | 0.34 | 7.5 | 0.72 |
| 10 | Kocaeli Turkey | 1999 | 53.7 | 0.21 | 7.5 | 1.41 |
| 11 | Landers | 1992 | 86 | 0.23 | 7.3 | 0.96 |
| 12 | Landers | 1992 | 82.1 | 0.40 | 7.3 | 1.10 |
| 13 | Loma Prieta | 1989 | 9.8 | 0.52 | 6.9 | 1.17 |
| 14 | Loma Prieta | 1989 | 31.4 | 0.57 | 6.9 | 0.94 |
| 15 | Manjil Iran | 1990 | 40.4 | 0.22 | 7.4 | 1.11 |
| 16 | Superstition Hills | 1987 | 35.8 | 0.38 | 6.5 | 0.86 |
| 17 | Superstition Hills | 1987 | 11.2 | 0.40 | 6.5 | 1.09 |
| 18 | Cape Mendocino | 1992 | 22.7 | 0.56 | 7 | 0.87 |
| 19 | Chi-Chi Taiwan | 1999 | 32 | 0.47 | 7.6 | 0.42 |
| 20 | Chi-Chi Taiwan | 1999 | 77.5 | 0.52 | 7.6 | 0.99 |
| 21 | San Fernando | 1971 | 39.5 | 0.21 | 6.6 | 2.23 |
| 22 | Friuli Italy | 1976 | 20.2 | 0.34 | 6.5 | 1.44 |

The spectral acceleration intensity at which 50% (22 ground motions) of the records result in the collapse of the structure is referred to as the median collapse capacity, or $S_{CT}$. Similarly, $CMR_{4\%}$ is the corresponding collapse margin ratio, and $S_{CT(4\%)}$ is the spectral acceleration intensity at which 50% (22 ground motions) of the records surpass the 4% interstory drift limit. The MCE ground motion response spectrum, or $S_{MT}$, is ascertained by:

$$S_{MT} = S_{MS} \qquad T \le T_s \tag{4}$$

$$S_{MT} = \frac{S_{M1}}{T} \qquad T \ge T_s \tag{5}$$

Since all archetypes were designed with the SDC $D_{max}$, $T_s$, $S_{M1}$, and $S_{MS}$ are taken as 0.6, 0.9, and 1.5 g, respectively, based on Table 6-1 of FEMA P695. The outcomes of the IDA analysis are reported in Table 4.

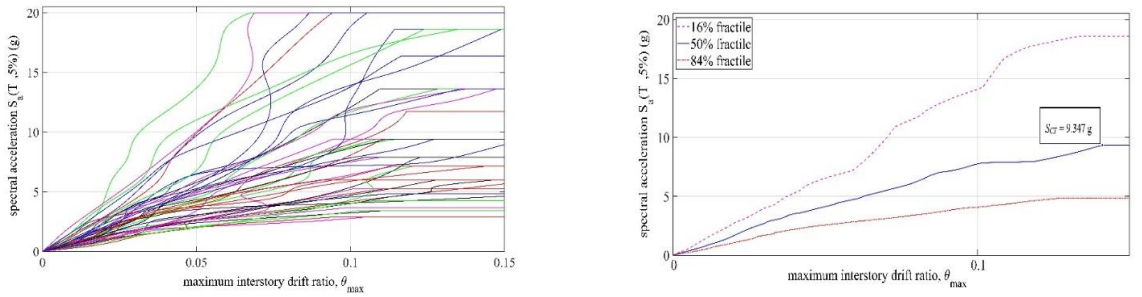


(a) 3-story frame

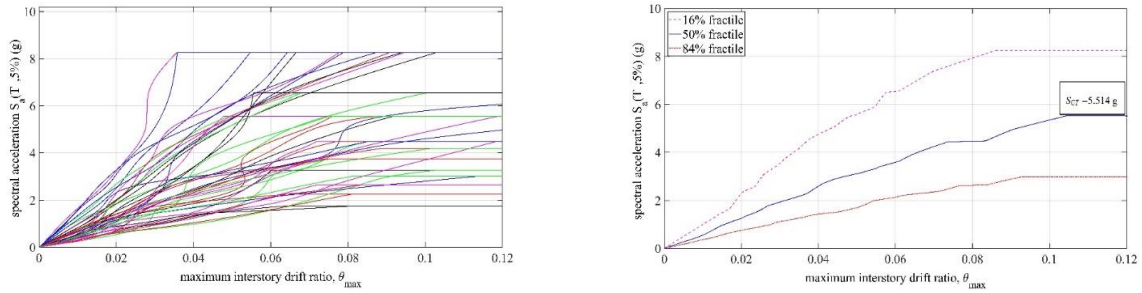


(b) 5-story frame

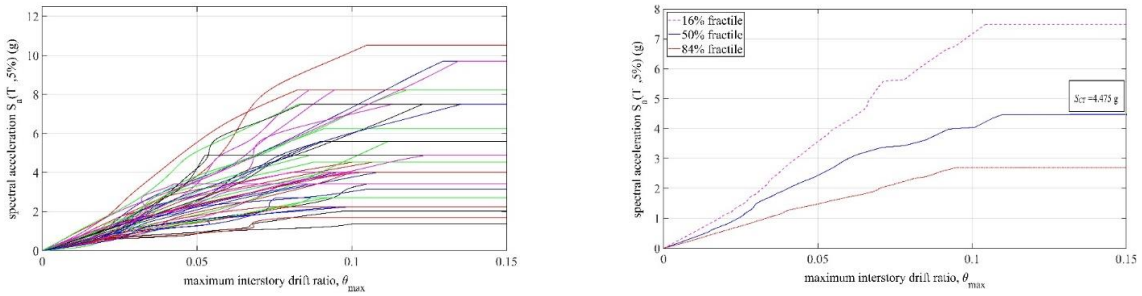


(c) 10-story frame

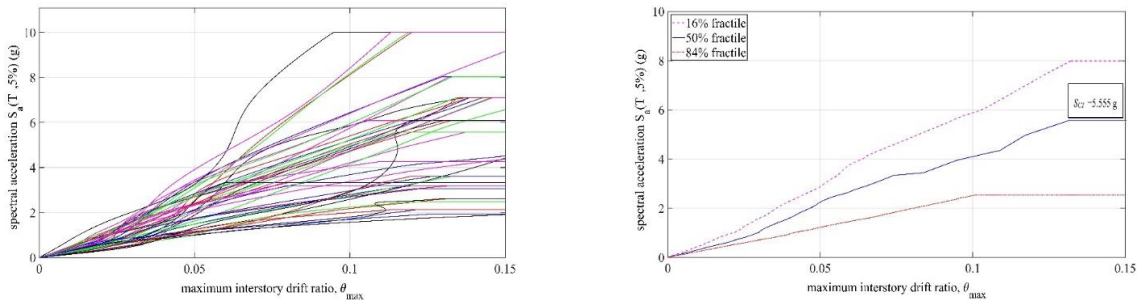


(d) 15-story frame

*Figure 7. IDA curves of RCS frames*

*Table 4. Results of the IDA analysis*

| Archetype | $T$ (sec) | $S_{M1}$(g) | $S_{MT}$(g) | $S_{CT}$(g) | $S_{CT\,(4\%)}$(g) | $CMR$ | $CMR_{(4\%)}$ |
|---|---|---|---|---|---|---|---|
| 3-story | 0.46 | 0.9 | 1.50 | 9.35 | 3.52 | 6.23 | 2.35 |
| 5-story | 0.67 | 0.9 | 1.34 | 5.51 | 2.61 | 4.10 | 1.94 |
| 10-story | 1.13 | 0.9 | 0.80 | 3.97 | 2.01 | 4.97 | 2.52 |
| 15-story | 1.53 | 0.9 | 0.59 | 5.56 | 1.62 | 9.44 | 2.75 |

Using a cumulative distribution function and the ground motion intensity collapse data, the fragility curves were also plotted. The fragility curves for the RCS frames are shown in Figure 8. The findings reveal that the 5-, 10-, and 15-story frames have larger collapse probabilities.

### 4.1 Collapse performance evaluation

As per FEMA P695, the CMR and $CMR_{4\%}$ values that were acquired from the IDA analysis must be modified by computing the adjusted collapse margin ratio, ACMR and $ACMR_{(4\%)}$, and by applying a spectral shape factor, SSF. The adjusted collapse margin ratio, ACMR and $ACMR_{(4\%)}$ is given by:

$$CMR(ACMR_{(4\%)}) = CMR(CMR_{(4\%)}).SSF \quad (6)$$

The SSF values for the different seismic design categories are provided by FEMA P695 Tables 7-1a and 7-1b, which are based on the fundamental period and ductility factor of the models. The uncertainties including record-to-record uncertainty, $\beta_{RTR}$, design requirements uncertainty, $\beta_{DR}$, test data uncertainty, $\beta_{TD}$, and modelling uncertainty, $\beta_{MDL}$, need to be quantified to calculate the total system collapse uncertainty, $\beta_{TOT}$, given by:

$$\sqrt{\beta_{RTR}^2 + \beta_{DR}^2 + \beta_{TD}^2 + \beta_{MDL}^2} \quad (7)$$

$\beta_{RTR}$ is determined as 0.4 for structures with a ductility factor greater than 3 in accordance with the FEMA P695 procedure. To ascertain the other uncertainties, a qualitative metric such as [(A) Superior, $\beta$ = 0.1, (B) Good, $\beta$ = 0.2, (C) Fair, $\beta$ = 0.35, (D) Poor, $\beta$ = 0.5] is employed. Seismic design was carried out in accordance with the guidelines given in ASCE/SEI 7-05 (2006) and FEMA P695 (2009) to account for design requirements uncertainty. The updated ASCE guidelines (Cordova 2005) were followed to design RCS composite joints. The reinforced concrete columns and steel beams were designed according to ACI 318-19 (2019) and AISC 360-16 (2016). Sufficient experimental research on RCS systems and their composite connections has been done to address test data uncertainty. In terms of modelling uncertainty, the RCS frames were modelled using the numerical model developed by Cordova (2005). Shear and bearing failures, the two primary failure mechanisms of RCS connections, can be well captured by this numerical model. The quality level of "fair" and the corresponding value of 0.35 were assigned for all uncertainties, resulting in a $\beta_{TOT}$ of 0.725 obtained from Eq. (7).

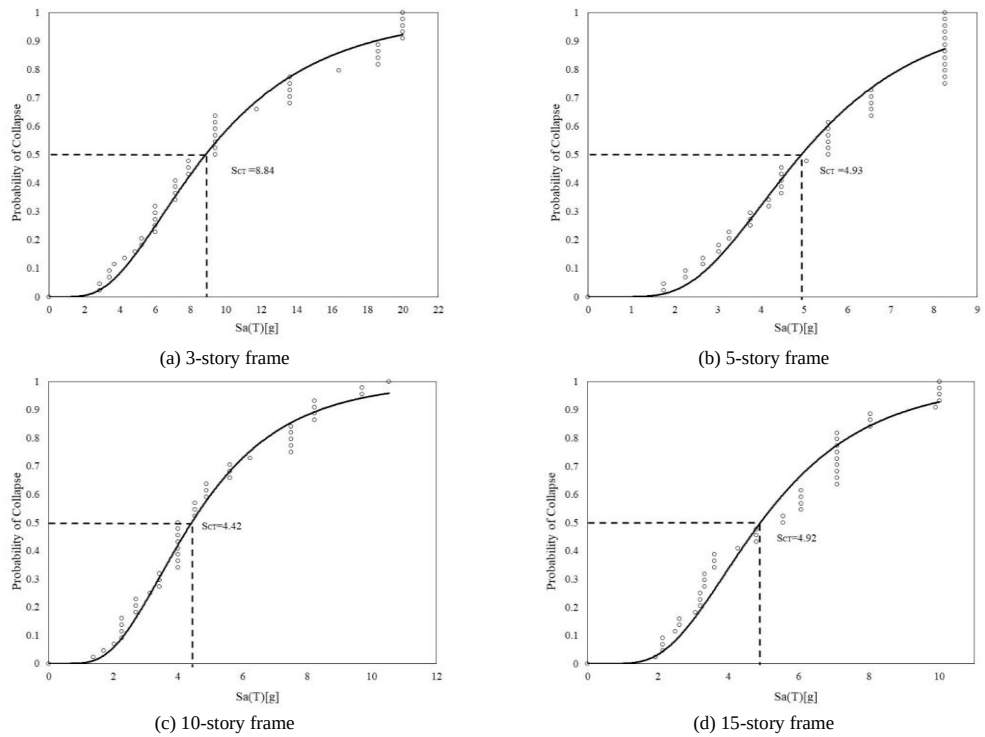


(a) 3-story frame (b) 5-story frame

(c) 10-story frame (d) 15-story frame

*Figure 8. Fragility curves of RCS frames*

*Table 5. Collapse performance evaluation (R = 8)*

| Archetype | *CMR* | $CMR_{(4\%)}$ | *SSF* | *ACMR* | $ACMR_{(4\%)}$ | $ACMR_{10\%}$ | $ACMR_{20\%}$ | Check |
|---|---|---|---|---|---|---|---|---|
| 3-story | 6.23 | 2.35 | 1.33 | 8.29 | 3.12 | 2.53 | 1.84 | Pass |
| 5-story | 4.10 | 1.94 | 1.37 | 5.62 | 2.66 | 2.53 | 1.84 | Pass |
| 10-story | 4.97 | 2.52 | 1.50 | 7.46 | 3.78 | 2.53 | 1.84 | Pass |
| 15-story | 9.44 | 2.75 | 1.61 | 15.20 | 4.43 | 2.53 | 1.84 | Pass |

FEMA P695 limits the average collapse probability of archetypes subjected to MCE ground vibrations to 10%. Furthermore, the collapse probability of a single archetype is capped at 20%. The FEMA P695 Table 7-3 provides the allowable values of the ACMR for various values of $\beta_{TOT}$. These values correspond to a 10% and 20% collapse probability, respectively, and depend on the amount of the uncertainties. The mean ACMR and ACMR of each archetype must be equal to, or greater than, $ACMR_{10\%}$ and $ACMR_{20\%}$, respectively. Based on $\beta_{TOT}$ =0.725, the acceptable values of $ACMR_{10\%}$ and $ACMR_{20\%}$ are 2.53 and 1.84, respectively. Table 5 summarizes the results of collapse performance assessment of the archetypes. The mean ACMR and $ACMR_{(4\%)}$ of the archetypes are 9.14 and 3.50, respectively, which are both greater than 2.53. As indicated in Table 5, the lowest ACMR and $ACMR_{(4\%)}$ are 5.62 and 2.66 (for the 5-story RCS frame), respectively, meaning that the ACMR and $ACMR_{(4\%)}$ of each archetype are also greater than the $ACMR_{20\%}$. As a result, all archetypes satisfy the performance requirements for both the 4% drift limit and global instability. The results show R factor of 8 given in IBC (2006) and ASCE/SEI 7-05 (2006) is conservative.

## 5 Conclusion

In accordance with the process described in FEMA P695, this study examined the seismic resilience, response modification factor and probability of collapse of RCS special moment frames. Incremental dynamic analyses were performed on multi-story (3-, 5-, 10-, and 15-story) RCS frames using a set of 44 ground motions that were specified in FEMA P695. Collapse fragility was also developed in order to evaluate the appropriateness of the collapse margin ratio of the archetypes. Throughout the process, different uncertainties were considered. Two failure criteria were applied: a global dynamic instability limit and a 4% interstory drift limit. The collapse performance evaluation of the archetypes was conducted with an R factor of 8, as recommended by IBC and ASCE/SEI 7-05 for special moment frames. All archetypes designed with R factor of 8 provided a reliable and conservative safety margin against collapse. The adjusted collapse margin ratio (ACCM) and $ACMR_{(4\%)}$ were compared to the allowable ranges suggested in FEMA P695. The mean value of ACMR (9.14) and $ACMR_{(4\%)}$ (3.50) of the archetypes were both greater than $ACMR_{10\%}$ value of 2.53. The results indicate that every archetype met the $ACMR_{20\%}$ requirements, with the lowest ACMR and $ACMR_{(4\%)}$ being 5.62 and 2.66, respectively. Following the recommendations in FEMA P695 procedure, future studies should investigate a larger R factor of 9 for RCS frames to evaluate the collapse margin ratio and seismic performance. Future research should also take into account the most recent RCS connection details recommended in the literature (Figure 1) to examine which RCS joint details results in better seismic performance of RCS frames in terms of CMR, as current study is restricted to typical RCS connection details with SBP and FBP (Figure 1.a).

## 6 References

ACI 318-19 (2019), *"Building Code Requirements for Structural Concrete"*, American Concrete Institute.

AISC, ANSI/AISC 360-16 (2016), *"Specification for structural steel buildings",* Chicago.

Alizadeh, S., Attari, N.K., and Kazemi, M.T. (2013). "The seismic performance of new detailing for RCS connections", *J. Constr. Steel Res.*, 91, 76-88.

Alizadeh, S., Attari, N.K., and Kazemi, M.T. (2015), "Experimental investigation of RCS connections performance using self-consolidated concrete", *J. Constr. Steel Res.*, 114, 204-216.

ANSI/AISC 341-10 (2010)*, "Seismic provisions for structural steel buildings*", Chicago.

ASCE 41-06 (2007)*, "Seismic rehabilitation of existing buildings*", American Society of Civil Engineers.

*ASCE 7-05* (2006), *"Minimum design loads for buildings and other structures*", American Society of Civil Engineers.

ASCE Task Committee (1994), *"Guidelines for design of joints between steel beams and reinforced concrete columns"*, *J. Struct. Eng.*, 120(8), 2330-2357.

Azar, B.F., Ghaffarzadeh, H., and Talebian, N. (2013), "Seismic performance of composite RCS special moment frames", *KSCE J. Civ. Eng.*, 17(2), 450-457.

Bracci, J.M., Jr, W.P.M., and Bugeja, M.N. (1999), "Seismic design and constructability of RCS special moment frames", *J. Struct. Eng.*, 125(4), 385-392.
Bugeja, M.N., Bracci, J.M., and Moore Jr, W.P. (2000), "Seismic behavior of composite RCS frame systems", *J. Struct. Eng.*, 126(4), 429-436.
Chen, C.-H., Lai, W.-C., Cordova, P., Deierlein, G.G., and Tsai, K.-C. (2004), "Pseudo-dynamic test of full-scale RCS frame: part I-design, construction, testing", *Structures Congress,* Nashville, May.
Chou, C.-C. and Chen, J.-H. (2010), "Tests and analyses of a full-scale post-tensioned RCS frame subassembly", *J. Constr. Steel Res.*, 66(11), 1354-1365.
Cordova, P., Chen, C.-H., Lai, W.-C., Deierlein, G.G., and Tsai, K.-C. (2004), "Pseudo-dynamic test of full-scale RCS frame: part II-analysis and design implications", *Structures Congress,* Nashville, May.
Cordova, P.P. (2005), "Validation of the seismic performance of composite RCS frames: full-scale testing analysis and seismic design", Ph.D. Dissertation, Stanford University.
Deierlein, G.G. (1988), "Design of moment connections for composite framed structures", Ph.D. Dissertation, The University of Texas, Austin.
Eghbali, N.B. and Mirghaderi, S.R. (2017), "Experimental investigation of steel beam to RC column connection via a through-plate", *J. Constr. Steel Res.*, 133, 125-140.
FEMA, P695 (2009)*, "Quantification of Building Seismic Performance Factors"*, Federal Emergency Management Agency, Washington, D.C.
Griffis, L.G. (1992), "Composite frame construction.", *Constructional steel design: an international guide*, 523-553.
Habashizadeh Asl, M.H., Chenaglou, M.R., Abedi, K., and Afshin, H. (2013), "3D finite element modelling of composite connection of RCS frame subjected to cyclic loading*", Steel and Comp. Struct.*, 15(3), 281-298.
Habashizadeh Asl, M.H. (2011), "Effects of isotropic and kinematic hardening on the RCS connection due to cyclic loading", *Int. J. Earth Sci. Eng.*, 4, 534-537.
International Code Council (ICC), (2006), "*International Building Code (IBC)*, Falls Church (VA).
Kanno, R. and Deierlein, G.G. (1996), "Seismic behavior of composite (RCS) beam-column joint subassemblies", *Composite construction in steel and concrete III*, ASCE.
Kanno, R. and Deierlein, G.G. (2002), "Design model of joints for RCS frames", *Composite construction in steel and concrete IV*, ASCE.
Kanno, R. (1993), "Strength, deformation, and seismic resistance of joints between steel beams and reinforced concrete columns", (Volumes I and II), Cornell University.
Kuramoto, H. and Nishiyama, I. (2004), "Seismic performance and stress transferring mechanism of through-column-type joints for composite reinforced concrete and steel frames", *J. Struct. Eng.*, 130(2), 352-360.
Li, W., Li, Q.-n., Jiang, W.-s., and Jiang, L. (2011), "Seismic performance of composite reinforced concrete and steel moment frame structures–state-of-the-art" *Comp. Part B: Eng.*, 42(2), 190-206.
Li, W., Xiong, J., Wu, L., and Yang, K. (2020), "Experimental study and numerical analysis on seismic behavior of composite RCS frames", *Struct. Conc.*, 21(5), 2044-2065.
Liang, X. and Parra-Montesinos, G.J. (2004), "Seismic behavior of reinforced concrete column-steel beam subassemblies and frame systems", *J. Struct. Eng.*, 130(2), 310-319.
Men, J., Zhang, Y., Guo, Z., and Shi, Q. (2015), "Experimental research on seismic behavior of a composite RCS frame", *Steel and Comp. Struct.*, 18(4), 971-983.
Nishiyama, I., Kuramoto, H., and Noguchi, H. (2004), "Guidelines: seismic design of composite reinforced concrete and steel buildings", *J. Struct. Eng.*, 130(2), 336-342.
Noguchi, H. and Uchida, K. (2004), "Finite element method analysis of hybrid structural frames with reinforced concrete columns and steel beams", *J. Struct. Eng.*, 130(2): 328-335.
Ou, Y. C., Nguyen, N. V. B., & Wang, W. R. (2022). Seismic shear behavior of new high-strength reinforced concrete column and steel beam (New RCS) joints. Engineering Structures, 265, 114497.
Parra-Montesinos, G. and Wight, J.K. (2001), "Modeling shear behavior of hybrid RCS beam-column connections", *J. Struct. Eng.*, 127(1), 3-11.
Parra-Montesinos, G., Liang, X., and Wight, J. (2003), "Towards deformation-based capacity design of RCS beam–column connections", *Eng. Struct.*, 25(5), 681-690.
Sheikh, T.M., Deierlein, G.G., Yura, J.A., and Jirsa, J.O. (1989), "Beam-column moment connections for composite frames: Part 1", *J. Struct. Eng.*, 115(11), 2858-2876.
Sheikh, T.M. (1987), "Moment connections between steel beams and concrete columns", The University of Texas, Austin.
Wu, Y., Xiao, Y., and Anderson, J. (2009), "Seismic behavior of PC column and steel beam composite moment frame with posttensioned connection", *J. Struct. Eng.*, 135(11), 1398-1407.